EARTHQUAKE ENGINEERING AND STRUCTURAL DYNAMICS
Earthquake Engng Struct. Dyn. 2001; **30**:173–193

Detection of soil liquefaction from strong motion records

Mladen V. Kostadinov and Fumio Yamazaki*,†

Institute of Industrial Science, University of Tokyo, 4-6-1 Komaba, Meguro-ku, Tokyo 153-8505, Japan

SUMMARY

During the recent earthquakes in Japan and the U.S.A. a number of records from liquefied-soil sites have been obtained. The ground motion parameters from these sites were studied and several methods for detection of liquefaction from seismic records were developed. The methods, however, focus mainly on the horizontal ground motion and may interpret as liquefaction-induced some records from soft-soil deposits or records with dominant surface waves, at which sites the phenomenon was not observed. Besides, not all of the available records from liquefied sites were processed. In this paper, after examination of the ability of different types of ground motion parameters to indicate alone soil liquefaction we propose a new liquefaction detection method that simultaneously analyses instantaneous frequency content of the horizontal and the vertical ground acceleration. We also compare performance of the proposed method with that of the other liquefaction detection methods. The computations are carried out using a common data set including records from liquefied and non-liquefied sites. Results show that the frequency-related parameters and the proposed method detect more efficiently the occurrence of liquefaction from the seismic records. Copyright © 2001 John Wiley & Sons, Ltd.

KEY WORDS: liquefaction detection; ground motion parameters; strong motion records; mean instantaneous frequency

1. INTRODUCTION

The 1994 Northridge earthquake in the U.S.A. and the 1995 Hyogoken-Nanbu (Kobe) earthquake in Japan corroborated the need for further development of earthquake monitoring and early damage assessment systems as a keystone of the earthquake disaster management. These systems collect information about the observed ground motion during or immediately after an earthquake and analyse it for the purpose of early warning and preliminary damage estimation. The backbone of such systems is a ground-motion monitoring network, consisting usually of three-axial accelerometers. Various national organizations, local governments and private companies in Japan and the U.S.A. have launched new seismometer networks or started to expand their existing ones as a part of real-time earthquake disaster mitigation systems [1]. Early

* Correspondence to: Fumio Yamazaki, Institute of Industrial Science, University of Tokyo, 4-6-1 Komaba, Meguro-ku, Tokyo 153-8505, Japan.
† E-mail: yamazaki@iis.u-tokyo.ac.jp

Received 4 January 2000
Revised 21 April 2000
Accepted 23 May 2000

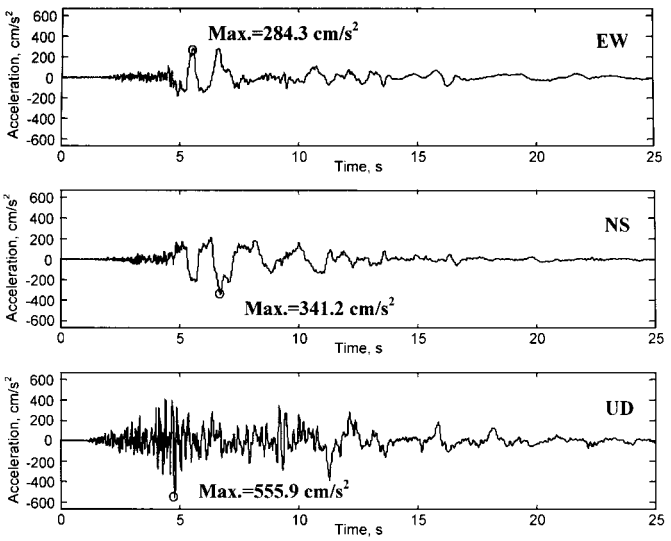

Figure 1. Acceleration record at Port Island GL from the 1995 Hyogoken-Nanbu earthquake. The site was heavily liquefied.

damage assessment systems within them can predict structural damage not only due to the ground shaking, but also due to fire, soil liquefaction or tsunami.

Since the 1964 Niigata earthquake, a number of ground motion records from liquefied-soil sites have been obtained. The records show that the horizontal ground acceleration alters uniquely after the onset of liquefaction — its frequency abruptly drops off to the range 0.5–1 Hz and its amplitudes decrease — while the vertical acceleration is rather stable (Figure 1). This alteration of the horizontal acceleration is triggered by the decreasing of the soil shear modulus as a consequence of the pore–water pressure buildup under undrained condition. An adequate description of the alteration can be used as a method for detection of liquefaction from the seismic records. Such a method can operate data from a seismometer network and identify the occurrence of the phenomenon immediately after an earthquake. It can also function as a standalone liquefaction sensor in combination with an accelerometer. Liquefaction has been recognized as the main reason for collapse of earth dams and slopes, failure of foundations, superstructures and lifelines and its early detection might be of great interest.

A practical approach to capture the alteration of ground motion is to calculate appropriate ground motion parameters and compare their values with limit ones that correspond to soil liquefaction. The advantages of this approach are that the alteration is expressed in terms of physically meaningful quantities and that computations are simple. The disadvantage is the incompleteness of the alteration description. Another possible approach is to perform nonlinear effective-stress analysis of the soil. This model-based approach is more comprehensive, but involves knowledge of soil properties, incident motion and complicated computations. Besides the surface accelerometers, other liquefaction detectors as downhole piezometers or sensors

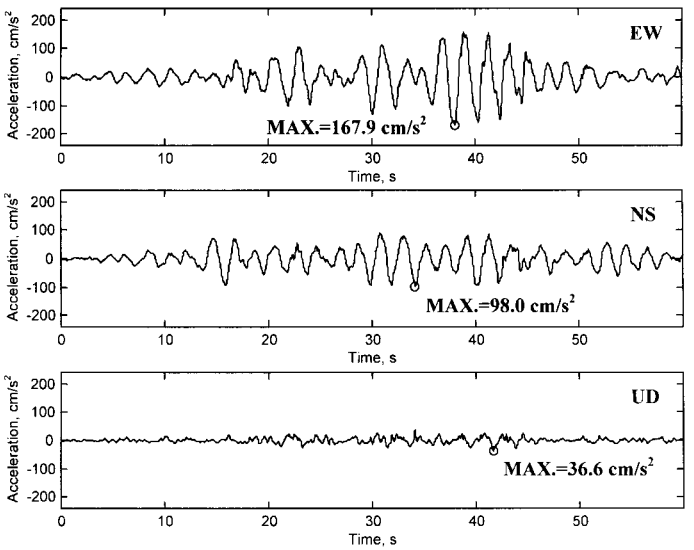

Figure 2. Acceleration record at SC&T from the 1985 Michoacan, Mexico earthquake. No liquefaction occurred at the site.

measuring the rise of the water level in a hollow pipe, inserted in the ground [2] could also be efficient. However, they are costly and with low durability.

The ground motion parameters from liquefied-soil sites were examined in a number of studies [3–9] and some of them were employed in several methods for liquefaction judgment from the strong motion records. Nakayama *et al.* [10] presented a method, which judges about the occurrence of liquefaction either positively or negatively. Miyajima *et al.* [11] proposed a three-level possibility method trying to distinguish some sites, where the liquefaction occurrence was questionable. Ozaki [12] introduced a simple method considering one parameter. These methods, however, focus mainly on the horizontal ground motion and may interpret as liquefaction-induced some records from soft-soil deposits or records with dominant surface waves, at which sites phenomenon was not observed. An example is the record at SC&T from the 1985 Michoacan, Mexico earthquake, shown in Figure 2. Besides, not all of the available records from liquefied-soil sites were processed.

In this paper, we first review existing methods for liquefaction detection from the seismic records. Then we examine the ability of the different ground motion parameters, employed in the liquefaction judgment methods, to indicate alone occurrence of the phenomenon and propose a new liquefaction detection method that simultaneously analyses the instantaneous frequency content of the horizontal and the vertical ground acceleration. Finally, we compare the performance of the proposed method with that of the other methods. All computations are carried out using a common data set of seismic records from liquefied and non-liquefied sites in Japan, the U.S.A. and Mexico. We also suggest a classification of the recording sites with respect to the liquefaction occurrence due to a particular earthquake.

2. REVIEW OF EXISTING METHODS FOR LIQUEFACTION DETECTION USING STRONG MOTION RECORDS

Existing methods for liquefaction detection are briefly reviewed in this section. The methods are named after the researchers who have proposed them.

2.1. Method of Suzuki

This method processes the two horizontal acceleration components and gives either positive or negative judgment about liquefaction occurrence. The method considers the following ground motion parameters:

(1) Peak horizontal ground acceleration (PGA). PGA is the maximal value of the vector sum of the two horizontal ground acceleration components. Results of Seed and Idriss [3] show that that the liquefaction occurrence is likely when the maximum ground surface acceleration is larger than $100\,\mathrm{cm/s^2}$.

(2) Maximum spectrum intensity ($SI_{\max}$). Definition of the spectrum intensity (SI) used here is

$$SI = \frac{1}{2.4}\int_{0.1}^{2.5} S_{\mathrm{v}}(T,\zeta)\,\mathrm{d}T \tag{1}$$

where S_{v} is the relative-velocity response spectrum of a single-degree-of-freedom system for a damping ratio ζ equal to 20 per cent of the critical one and T is the undamped period of vibration. Towhata *et al.* [6] found that *in situ* liquefaction is unlikely to occur when surface SI is less than $13\,\mathrm{cm/s}$. The maximum value of the spectrum intensity $SI_{\max}$ is obtained by rotating the horizontal acceleration in eight directions equally spaced between 0 and 180°.

(3) Maximum horizontal ground displacement (D_c). Towhata *et al.* [6] suggested the maximum horizontal ground displacement to be computed as

$$D_c = \frac{2SI^2}{PGA} \tag{2}$$

Here D_c is the displacement due to the harmonic vibration and does not represent the permanent displacement of the liquefied soil. It was found that in the case of liquefied sites D_c takes relatively large values.

(4) Zero-crossing period ($T_{\mathrm{z,a}}$). It is defined as

$$T_{\mathrm{z,a}} = \frac{2T}{n} \tag{3}$$

where T is the interval of time and n is the number of acceleration zero-crossings. The zero-crossing period is calculated within a 10-s window that moves with step of 1 s in the time interval between occurrence of peak acceleration and 10 s after it. Then the greatest among the obtained 10 values is found out. Finally $T_{\mathrm{z,a}}$ is determined as the larger of the maximal zero-crossing periods of the two horizontal acceleration components.

Occurrence of liquefaction is judged if all parameters exceed certain limit values: (1) $PGA \geqq 100$ cm/s^2, (2) $SI_{\max} \geqq 20$ cm/s, (3) $D_c \geqq 10$ cm and (4) $2T_{z,a} \geqq 2$ s.

The method of Suzuki is implemented into new SI sensor, developed by Tokyo Gas Co., Ltd. The company plans to install 3600 pieces of this sensor as a part of its real-time disaster mitigation system SUPREME [13].

2.2. *Method of Miyajima*

This method analyses the three components of an accelerogram. It distinguishes three possibilities for liquefaction in attempt to identify some cases where the occurrence of liquefaction was not clear. The method evaluates the following four parameters (computation of some of them is modified as in Yamamoto *et al.* [14]:

(1) Maximal ratio of vertical to horizontal acceleration amplitude ($A_{V,\max}/A_{H,\max}$). Acceleration time history is divided into portions of 0.3 s and the ratio is composed from the largest vertical and horizontal amplitude in each portion. It was found that at liquefied sites the maximum of this ratio after occurrence of PGA is larger than 2.0.

(2) Ratio of low-frequency portion to whole area of the Fourier amplitude spectrum (R_L). Low-frequency portion and whole area of Fourier spectrum are defined as the areas under the Fourier amplitude spectrum curve from 0 to 2 Hz and from 0 to 10 Hz, respectively. The value of R_L indicates the amount of low-frequency motion in the horizontal acceleration components. In this study R_L is the average of the two ratios that correspond to the two horizontal components.

(3) Averaged predominant frequency ($F_{p,a}$). Predominant frequency is the frequency corresponding to the maximum value of the (usually smoothed) Fourier amplitude spectrum. The time history of the predominant frequency for each horizontal acceleration component is calculated using a moving window of length 5 s that moves with a step of 0.5 s. Then the average value of the resultant time history is obtained within the time interval between occurrence of the peak acceleration and the time where the greatest amplitude of the Fourier spectrum becomes less than 10 cm/s. Finally $F_{p,a}$ is determined as the mean of the two average values related to each horizontal acceleration component. At liquefied sites $F_{p,a}$ is found not to exceed 1 Hz.

(4) Maximal decrease rate of the predominant frequency ($\Delta F_{p,\max}$). Decrease rate is defined as the negative rate of change. The rate of change of the predominant frequency is the difference of its two consecutive values, divided on the time lag between them. In this study $\Delta F_{p,\max}$ is the average of the two maximal decrease rates that correspond to the two horizontal components.

Liquefaction occurrence is judged using a point system. In case that any of the parameters exceeds a limit value, points are given as follows: $A_{V,\max}/A_{H,\max} \geqq 2.0$ — 1 point, $R_L \geqq 0.25$ — 1 point, $F_{p,a} \leqq 1$ Hz and $\Delta F_{p,\max} \leqq 1$ Hz/s — 1 point, $F_{p,a} \geqq 1$ Hz and $\Delta F_{p,\max} < 1$ Hz/s — 0.5 points. If the sum of the points is less than 2.0, the possibility for liquefaction is judged as low. If the sum of points is equal or greater than 2.0 but less than 3.0, the possibility for liquefaction is determined as high and if the sum of points is equal to 3.0, the possibility for liquefaction is judged as very high.

2.3. Method of Ozaki and Takada

This method processes the two horizontal acceleration components. It takes into account one parameter — ratio of Arias intensity of filtered to non-filtered acceleration time history (R_I). Arias intensity (I_{xx}) is defined as [15]

$$I_{xx} = \frac{\pi}{2g} \int_0^{T_0} a_x^2(t)\,\mathrm{d}t \tag{4}$$

where $a_x(t)$ is the ground acceleration time history along the x-axis, T_0 is its duration, g is the gravity constant and t denotes the time. Considering the Parseval's formula one can notice that R_I indicates the low-frequency content of the power spectrum of the ground acceleration, i.e. it has same meaning as R_L. The filter used in this method is a low-pass filter with cut-off frequency of 1 Hz.

Occurrence of liquefaction is judged according to the value of R_I as follows: $0 = R_I < 0.3$ — no liquefaction, $0.3 \leqq R_I < 0.6$ — possible liquefaction, $0.6 \leqq R_I \leqq 1$ — liquefaction.

3. COMMON DATA SET OF STRONG MOTION RECORDS

In order to compare the performance of the individual ground motion parameters as well as that of the liquefaction detection methods a common data set of seismic records is developed. In this study, we concentrate on free-field records with *PGA* larger than 150 cm/s^2 and peak ground velocity (*PGV*) bigger than 15 cm/s though some downhole and structure records are presented.

The fact whether a record is from a liquefied site is judged from a report about the site condition after a particular earthquake. Liquefaction occurrence is proved by field evidence like sand boils, ground fissures filled with sand, large permanent displacements or vertical settlements of the soil, uplifting of pipelines or tanks, tilting of buildings, some foundation failures, etc. Seed *et al.* [16] pointed out that the liquefaction evidence takes different forms for different soils and suggested to consider two phenomena — 'liquefaction' and 'cyclic mobility'. The former involves very large deformations while the latter involves limited amount of cyclic strain in the soil. Depending on the soil profile, however, some liquefaction evidence such as sand boils may not be observed on the surface, when liquefaction occurs in depth [17].

In accordance with the above considerations, we classified the recording sites with respect to the liquefaction occurrence due to a particular earthquake in the following three groups:

(1) *Liquefied sites*: there was evidence seen for liquefaction at the recording site.
(2) *Liquefaction-suspicious sites*: there was no evidence seen for liquefaction at the recording site, but it was observed in its vicinity (up to 50 m) or cyclic mobility at the site was confirmed by an analytical study.
(3) *Non-liquefied sites*: there was no evidence for liquefaction at the recording site and its vicinity (up to 50 m) as well as no conformation about cyclic mobility at the site.

The common data set consists of 74 free-field, six downhole and three structure ground motion records from Japan, the U.S.A. and Mexico. American records are obtained from the Earthquake Strong Motion CD-ROM, National Geographical Data Centre [18] and from the Internet site of California Strong Motion Instrumentation Program (CSMIP). The early Japanese data are also obtained from the mentioned CD-ROM and the rest are provided by many

national organizations, institutes and private companies, including Japan Meteorological Agency (JMA), Port and Harbour Research Institute (PHRI), Ministry of Transport, Public Works Research Institute (PWRI), Ministry of Construction, Kyoshin net (K-net), National Research Institute of Earth Science and Disaster Prevention, etc.

For the purposes of the study, the records in the data set are divided in four categories: liquefied-site free-field (LF), liquefied-site structure (LS), suspicious-site free-field (SF) and non-liquefied-site free-field (NF). In total 12 liquefied-site records (LF and LS) and five suspicious-site free-field records are confirmed [19–31] (the information about Amagasaki bridge is collected by contacting PWRI). The record from Treasure Island during the 1989 Loma Prieta earthquake is classified as SF although the observations of liquefaction were 'within 100 m' of the seismic station [23]. The sudden amplitude decrease in the horizontal acceleration around 15 s from its beginning is associated with the liquefaction onset [32]. The record from Rokko Island, which site is liquefaction-suspicious [29], is put in the LS category. The downhole records GL-16 m and GL-32 m at Port Island from the 1995 Hyogoken-Nanbu earthquake are included in the LF and SF category, respectively, taking into account the analytical studies that estimate the possible liquefied layers in depth at that site [31]. This collection of records from liquefied sites claims to be the most comprehensive one examined by now. The non-liquefied free-field records are 66, including four downhole records from some liquefied, suspicious and non-liquefied sites. Table I shows all records in the data set and the corresponding values of *PGA* and *PGV*. Note that it was the 1995 Hyogoken-Nanbu earthquake from which most of the liquefied-site records are obtained.

A comment on the structure records is needed. This type of records is not used in the preliminary damage assessment, but it is put into consideration because all three sites were liquefied or liquefaction-suspicious. The Kawagishi-cho record is the first ever one obtained from a liquefied site. The seismometer was placed in the basement of a four-storey apartment building with a shallow foundation, next to the three tilted buildings at that site. The instrument at Kobe Dai 8 is installed on a quay wall and perhaps followed closely the movements of the ground. The seismometer at Rokko Island is located in the basement of a 40-storey building, founded with piles of depth 12 m. There are more instruments at the upper levels of this building, but their records follow the structure response.

4. ANALYSIS OF THE GROUND MOTION PARAMETERS USED IN THE METHODS FOR LIQUEFACTION DETECTION FROM SEISMIC RECORDS

Liquefaction detection methods discussed are successful combinations of selected ground motion parameters that distinguish liquefied-site records from these from non-liquefied sites. Efficiency of the method depends on efficiency of the parameters employed. Hence, it is important to grasp the ability of the different parameters to indicate alone soil liquefaction. Commonly, ground motion parameters are divided into four categories: amplitude-, frequency-, energy- and duration-related ones [17]. Figure 3 illustrates the parameters used in the methods for liquefaction detection with respect to the above classification. One can see that although the duration of the ground motion is influential to liquefaction occurrence, it is not considered as an efficient indicator.

Ability of the ground motion parameters employed in the liquefaction judgment methods to indicate alone soil liquefaction is analysed using both liquefied- and non-liquefied-site records

Table I. Seismic records used in this study.

No.	Site	PGA			PGV	Record type*	Lique-faction	Reference for lique-faction
		EW (cm/s^2)	NS (cm/s^2)	UD (cm/s^2)	Vector sum (cm/s^2)	Vector sum (cm/s)			
	Niigata Earthquake 16/06/1964								
1	Kawagishi-cho	170.86	128.92	55.84	186.06	65.1	S	LIQ	[19]
	Tokachi-Oki Earthquake 1/05/1968								
2	Aomori Harbor	196.53	227.31	156.38	275.91	39.9	F	LIQ	[20]
3	Hachinohe Harbor	206.21	311.73	135.45	312.76	39.1	F	NON	
4	Muroran Harbor	155.35	221.50	113.36	229.62	35.7	F	NON	
	Miyagiken-Oki Earthquake 12/06/1978								
5	Shiogama Harbor	288.17	314.33	213.86	316.12	53.6	F	NON	
	Nihonkai-Chibu Earthquake 26/05/1983								
6	Akita-S	205.45	190.09	40.93	222.42	37.4	F	NON	
7	Hachirogata	144.36	165.51	131.84	177.36	72.9	F	LIQ	[21]
	Michoacan, Mexico Earthquake 19/09/1985								
8	C. de Abastos Frigorifico	94.62	80.53	27.24	109.68	38.3	F	NON	
9	Caleta de Campo	138.49	137.84	88.35	140.14	20.7	F	NON	
10	SC&T	167.92	97.97	36.64	187.61	63.6	F	NON	
11	Tacubaya, D.F.	33.23	34.40	19.16	36.97	10.4	F	NON	
12	Tlahuac Bombas	106.67	135.88	23.98	137.90	68.6	F	NON	
	Superstition Hills Earthquake 24/11/1987								
13	Wildlife GL	179.52	201.15	414.81	206.60	30.6	F	LIQ	[22]
14	Wildlife GL −7.5	103.29	168.63	99.67	175.52	22.0	D	NON	
	Chibaken-Toho-Oki Earthquake 17/12/1987								
15	Chiba Array, IIS	213.60	327.06	124.77	329.33	15.5	F	NON	
16	Katsuura (KT552), NIED	189.38	209.04	131.88	257.34	25.4	F	NON	
17	Kisarazu (KT521), NIED	357.44	384.35	62.05	403.56	30.9	F	NON	
18	Mobara, Stokogyo	419.72	361.87	132.18	475.65	35.3	F	NON	
19	Narashino, Takenaka ED	151.87	242.63	97.21	242.63	9.1	F	NON	

Table I. *Contd.*

No.	Site	PGA				PGV	Record type*	Lique-faction	Reference for lique-faction
		EW (cm/s^2)	NS (cm/s^2)	UD (cm/s^2)	Vector sum (cm/s^2)	Vector sum (cm/s)			
	Loma Prieta Earthquake 18/10/1989								
20	Agnew, Agnews State Hospital	157.57	163.08	82.25	178.44	31.6	F	NON	
21	Capitola, Fire Station	390.79	462.92	500.05	541.69	41.1	F	NON	
22	Corralitos, Eureka Canyon Rd.	469.38	617.70	431.06	634.07	56.6	F	NON	
23	Emeryville, 6363 Christie Ave	254.69	210.33	58.52	255.53	45.2	F	NON	
24	Foster City, Redwood Shores	277.61	252.63	100.99	297.60	46.9	F	NON	
25	Gilroy #1, Gavilan College	433.62	426.61	206.36	436.07	39.2	F	NON	
26	Hollister, South St and Pine Drive	174.55	361.90	193.21	364.93	62.5	F	NON	
27	Santa Cruz, UCSC/Lick Lab.	401.54	433.12	324.57	491.95	22.1	F	NON	
28	Saratoga, Aloha Ave.	316.19	494.45	353.35	497.30	56.3	F	NON	
29	SF, International Airport	325.80	230.77	63.31	378.08	34.3	F	NON	
30	SF, Presidio	194.87	97.91	56.22	195.59	34.4	F	NON	
31	Treasure Island	155.85	97.94	15.86	158.72	34.3	F	SUS	[23]
	Kushiro-Oki Earthquake 15/01/1993								
32	Hanasaki-F	158.37	146.92	93.29	169.96	9.7	F	NON	
33	Kushiro, JMA	919.13	814.72	465.33	1024.07	71.2	F	NON	
34	Kushiro-G	343.93	467.78	342.40	467.82	62.1	F	SUS	[24]
35	Kushiro-GB	264.58	204.43	109.54	280.85	19.5	D	NON	
36	Nemuro, JMA	215.73	195.88	85.63	216.10	12.8	F	NON	
37	Tokachi-M	319.51	406.38	223.65	408.76	19.3	F	NON	
38	Urakawa, JMA	264.68	224.43	65.12	281.82	29.4	F	NON	
39	Urakawa-S	170.22	317.14	87.87	322.09	21.2	F	NON	
	Hokkaido-Nansei-Oki Earthquake 12/07/1993								
40	Hakodate-F	115.14	118.28	61.53	144.85	33.2	F	NON	
41	Hakodate-FB	59.75	71.00	45.87	71.01	16.4	D	NON	
42	Hakodate-M	148.80	145.42	87.25	151.79	32.4	F	NON	
43	Suttsu, JMA	202.18	215.97	50.98	216.65	16.0	F	NON	
	Northridge Earthquake 17/01/1994								
44	LA, Bell Postal Facility, Ground	154.20	260.35	81.64	272.63	17.4	F	NON	
45	LA, Griffith Observatory	291.10	163.78	142.92	291.94	28.5	F	NON	

Table I. *Contd.*

No.	Site	PGA				PGV	Record type*	Lique-faction	Reference for lique-faction
		EW (cm/s^2)	NS (cm/s^2)	UD (cm/s^2)	Vector sum (cm/s^2)	Vector sum (cm/s)			
46	LA, Sepulveda Canyon, Ground	462.06	257.63	150.34	470.11	28.3	F	NON	
47	LA, Wadsworth VA Hosp., South	297.95	382.94	144.96	471.31	39.2	F	NON	
48	Newhall, LA County Fire Station	571.62	578.19	537.35	731.84	119.1	F	NON	
49	Pasadena, 535 South Wilson Ave.	141.08	161.41	102.63	161.80	10.9	F	NON	
50	Tarzana, Cedar Hill Nursery	1744.53	970.74	1027.51	1965.20	114.7	F	NON	
51	Topanga, Fire Station, Ground	193.65	326.52	201.17	358.81	17.7	F	NON	
52	Santa Monica City Hall, Ground	865.97	362.62	227.67	866.34	41.7	F	NON	
53	Sylmar County Hospital	592.64	826.76	524.99	827.35	131.2	F	NON	
	Hokkaido-Toho-Oki Earthquake 04/10/1994								
54	Kushiro, JMA	473.38	454.96	192.92	561.31	37.6	F	NON	
55	Nemuro, JMA	330.33	369.05	183.48	414.02	31.4	F	NON	
56	Tomakomai, JMA	81.13	102.80	30.09	105.45	10.4	F	NON	
57	Urakawa, JMA	144.48	114.82	38.90	181.06	15.4	F	NON	
	Sanriku-Haruka-Oki Earthquake 28/12/1994								
58	Hachinohe, JMA	488.39	602.31	94.11	673.32	31.9	F	NON	
	Hyogoken-Nanbu Earthquake 17/01/1995								
59	Amagasaki Bridge GR-2	293.90	264.64	324.02	340.68	57.4	F	SUS	†
60	Amagasaki-G	498.51	324.24	310.32	499.56	61.5	F	LIQ	[25]
61	Amagasaki No.3 P.P., KE	353.62	226.63	373.38	366.00	58.9	F	LIQ	[26]
62	Gen. Tech. Research Inst. GL, KE	647.50	298.60	205.04	687.51	58.1	F	NON	
63	Higashi-Kobe Bridge	280.72	327.31	394.84	411.52	99.2	F	LIQ	[27]
64	Inagawa GR-1, PWRI	417.26	421.56	361.35	467.95	41.1	F	NON	
65	Kobe, JMA	617.34	818.01	332.24	847.88	105.3	F	NON	
66	Kobe-Dai8-G	389.58	686.09	341.32	726.63	189.4	S	LIQ	[28]
67	Kobe-JI-S	229.73	524.78	445.87	583.30	110.9	F	LIQ	[29]
68	Kobe University, CEORKA	307.69	276.06	454.37	324.24	57.2	F	NON	
69	JR Nishi Akashi Station	454.75	473.70	380.14	506.99	47.8	F	NON	
70	Port Island GL	284.34	341.22	555.91	426.54	103.2	F	LIQ	[30]

Table I. *Contd.*

No.	Site	PGA				PGV	Record type*	Lique-faction	Reference for lique-faction
		EW (cm/s^2)	NS (cm/s^2)	UD (cm/s^2)	Vector sum (cm/s^2)	Vector sum (cm/s)			
71	Port Island GL-16	543.19	564.88	789.59	636.79	88.4	D	LIQ	[31]
72	Port Island GL-32	461.72	543.59	200.00	713.22	85.0	D	SUS	[31]
73	Port Island GL-83	302.59	678.78	186.69	723.22	72.9	D	NON	
74	Rokko Island City, B3, B1F	195.59	319.56	507.75	386.03	74.8	S	SUS	[29]
75	Shin Kobe S.S., KE	584.25	510.73	495.33	688.11	102.6	F	NON	
76	Tadaoka, CEORKA	190.99	290.01	129.19	293.16	24.7	F	NON	
77	JR Takarazuka Station	683.63	600.94	418.20	690.44	97.6	F	NON	
78	JR Takatori Station	656.98	605.55	279.31	742.74	156.8	F	SUS	[29]
79	Yotsubahsi GR-1, PWRI	329.60	251.63	223.06	362.33	30.5	F	NON	
	Kagoshimaken-Hokuseibu Earthquake 13/05/1997								
80	Akune (KGS004)	124.98	155.81	99.67	173.46	18.5	F	NON	
81	Miyanojoh (KGS005)	901.05	902.10	287.59	976.57	46.8	F	NON	
82	Ohkuchi (KGS003)	176.32	172.08	63.94	187.45	10.3	F	NON	
83	Sendai (KGS007)	317.53	300.46	149.39	340.30	32.2	F	NON	

*S — Structure, F — Free field, D — downhole,
**LIQ — liquefied, SUS — suspicious, NON — non-liquefied.
†Contacted PWRI.

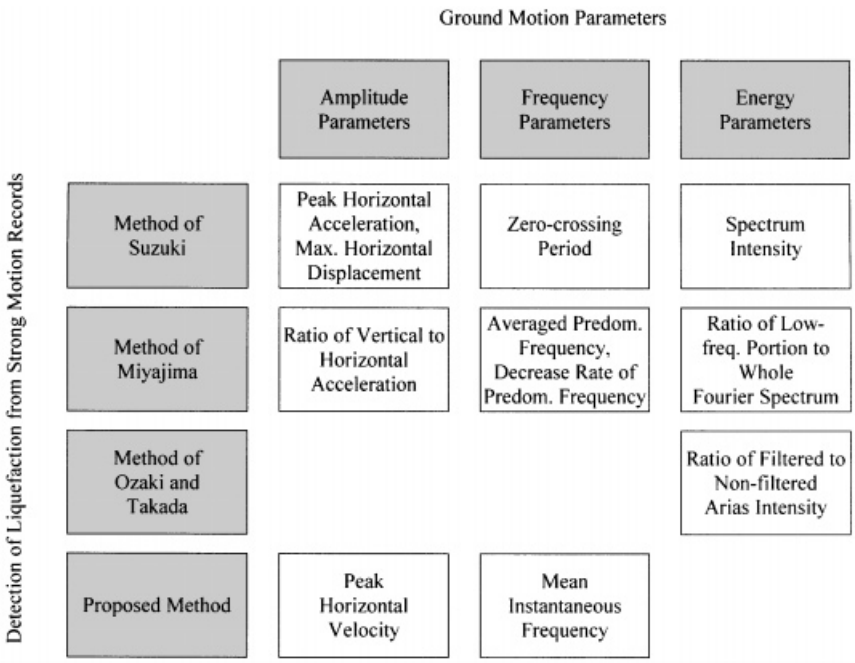

Figure 3. Ground motion parameters employed in the liquefaction detection methods.

from the common data set. It is assumed that a parameter detects liquefaction occurrence for a particular record if its value is within the range, specified in the corresponding method (e.g. $PGA \geqq 100\,\mathrm{cm/s^2}$ as in the method of Suzuki). Accordingly, same parameter detects no liquefaction if its value is out of that range (e.g. $PGA < 100\,\mathrm{cm/s^2}$). The representative value of R_I is assumed the larger from the two ratios that correspond to the two horizontal acceleration components and its range is selected to be $R_\mathrm{I} \geqq 0.3$. Decrease rate of the predominant frequency is not examined.

Figure 4(a) depicts the performance of the amplitude parameters. Because of the data set, *PGA* shows almost no efficiency in the detection of the NF records. However, its threshold picks all records from liquefied and liquefaction-suspicious sites. Best recognition is given by D_c that distinguishes almost two-thirds of the records from non-liquefied sites and all LF and SF records. $A_{\mathrm{V,max}}/A_{\mathrm{H,max}}$ detects even better the NF records but cannot identify one suspicious-site and one liquefied-site record. This might be because of the variation of that parameter with the starting point of its computation.

The results for the energy parameters are given in Figure 4(b). These parameters indicate all LF, LS and SF records. R_I recognizes 75 per cent of the records from non-liquefied sites while $SI_{\max}$ and R_L identify less than the half of them. The efficiency of R_I and R_L implies that some power spectrum characteristics might reflect better liquefaction occurrence than the corresponding Fourier spectrum ones.

Figure 4(c) illustrates the outcomes of the frequency parameters. All of them detect more than three-quarters of the records from non-liquefied sites and almost all LF, LS and SF records. $F_{\mathrm{p,a}}$ shows lower identification ability for the NF records and does not recognize one

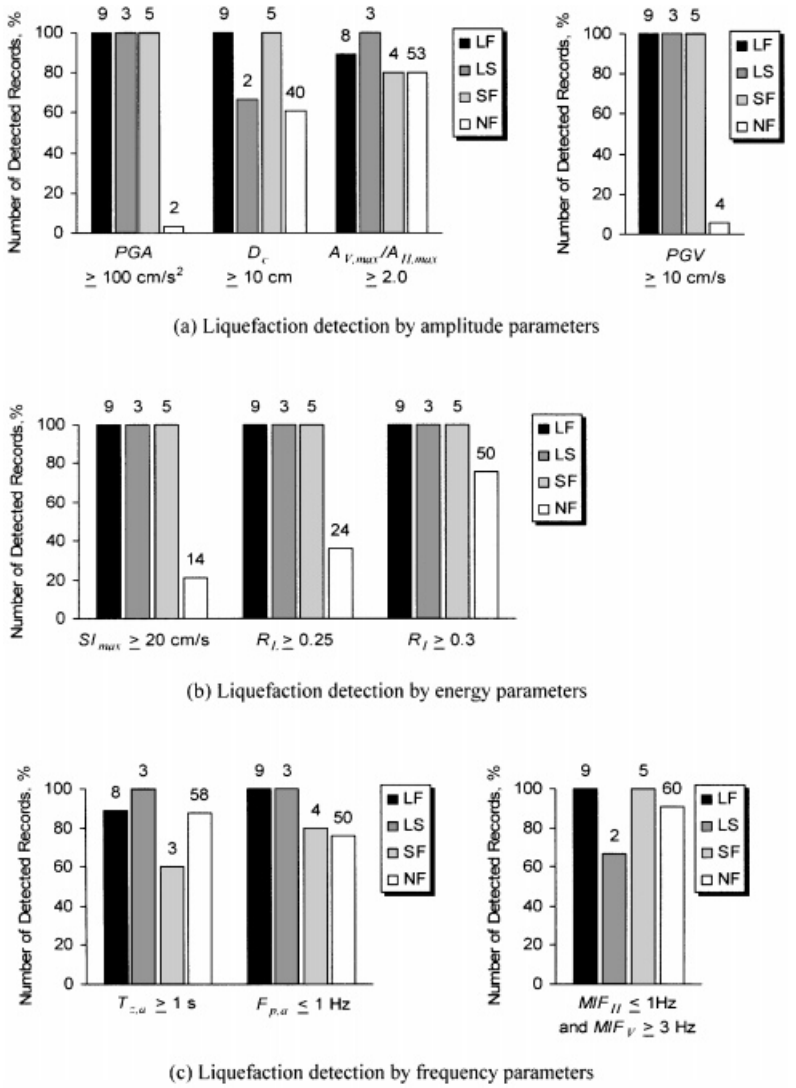

Figure 4. Detection of liquefaction occurrence by different ground motion parameters.

SF record. $T_{z,a}$ gives better detection of the NF records but does not identify one LF and two SF records. Both $F_{p,a}$ and $T_{z,a}$ are determined through the moving-window technique and have a threshold of 1 Hz (also found in computation of R_I).

From the analysis, it is seen that the frequency-related parameters are the most efficient among the three groups ground motion parameters employed in the detection of liquefaction occurrence. Frequency parameters are always combined with amplitude or energy parameters, which measure the ground-shaking intensity that is related to the magnitude of liquefaction-inducing stresses in the soil. Energy parameters should be applied carefully since they reflect

several characteristics of the ground motion and the effect of one parameter could be obscured by the effect of another.

5. PROPOSAL FOR A METHOD FOR LIQUEFACTION DETECTION FROM STRONG MOTION RECORDS

All methods for liquefaction detection, described in Section 2, focus on the frequency content of the horizontal ground motion. However, the main feature of the liquefied-site records is not only that the high-frequency content vanishes in the horizontal components of the accelerogram, but also that it exists at the same time in the vertical component. This is explained with the fact that the seismic body waves typically arrive at the ground surface from a nearly vertical direction. Therefore, we suggest analysing the instantaneous frequency behaviour of both horizontal and vertical acceleration simultaneously.

The instantaneous frequency behaviour of a given signal, i.e. how the signal frequency changes over the time is the subject of the joint time–frequency analysis. Taking the Fourier transform within a moving window, known also as short-time Fourier transform (STFT) is the simplest among the variety of time–frequency representations [33]. Its square, named STFT spectrogram is the most used time-dependent power spectrum. Another popular time–frequency methods are Wigner–Ville distribution and its derivatives — Cohen's class distributions.

In our proposal, we consider the mean instantaneous frequency (*MIF*) defined as

$$MIF(t) = \frac{\int f P(t, f)\, \mathrm{d}f}{\int P(t, f)\, \mathrm{d}f} \tag{5}$$

where $P(t, f)$ is a time–frequency representation of the acceleration time history, t is the time and f is the frequency. As a time–frequency representation is used the STFT spectrogram. In other words, we compute the mean frequency of the power spectrum of the moving window. Because it is a weighted average of all frequencies present at a given moment, *MIF* can quantify the frequency alternation in the ground acceleration records from liquefied sites. In the STFT computation a Hamming window of length 256 points is utilized for the acceleration records with a time increment of 0.01 s. For different time increments, the window length is changed proportionally in order to maintain similar frequency resolution (i.e. 128 points for time increment of 0.02 s). The window is moved stepwise within the time interval between the first and last exceeding of 40 $\mathrm{cm/s^2}$ of the horizontal acceleration. Figure 5 shows the *MIF* of the Higashi-Kobe bridge record during the 1995 Hyogoken-Nanbu earthquake.

Having the *MIF* computed, we detect the time instants at which it has relatively low value in any of the horizontal acceleration components and relatively high value in the vertical acceleration component. The total duration of this state (represented by the number of the time instants, multiplied by the time increment) is considered as an indicator for soil liquefaction. *MIF* limit values are determined empirically. The limit frequency for the vertical acceleration is set to 3 Hz. In order to distinguish the liquefied-site records form these from liquefaction-suspicious sites it is assumed that the frequency drop in the former is larger than the frequency drop in the latter. Respectively, two limits for the horizontal acceleration are introduced — 2/3 Hz for the records from liquefied sites and 1 Hz for the records from suspicious sites. The minimum total duration of low *MIF* in the horizontal acceleration component and high *MIF* in the vertical component is set to 0.1 s.

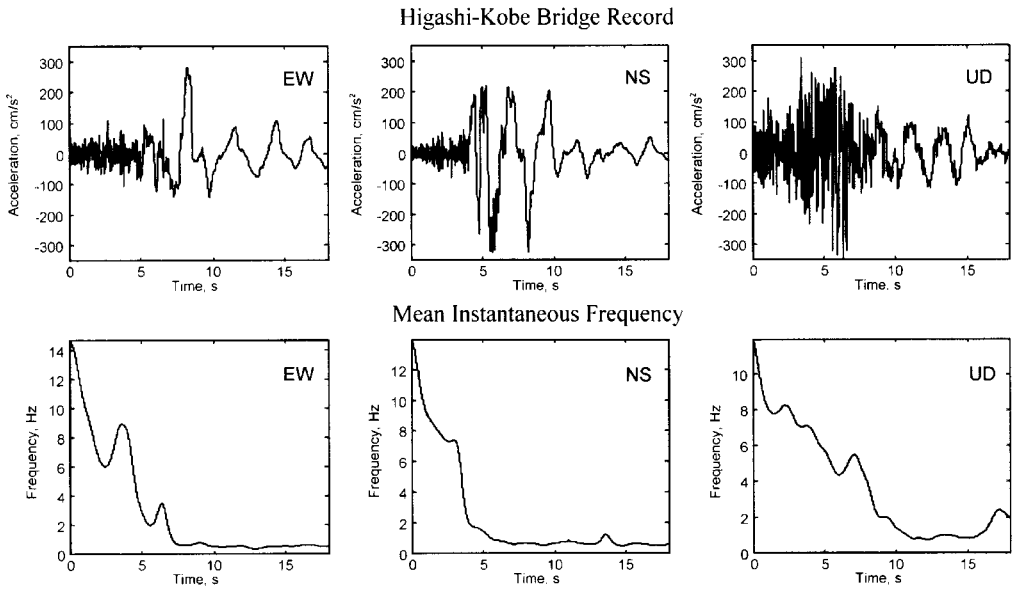

Figure 5. Mean instantaneous frequency of the Higashi-Kobe bridge record from the 1995 Hyogoken-Nanbu earthquake.

In addition to *MIF*, we employ in our method the peak horizontal ground velocity (*PGV*) defined as the maximal value of the vector sum of the two horizontal ground velocity components. Midorikawa and Wakamatsu [4] calculated the intensities of the ground motion at liquefied sites during past earthquakes by a semi-empirical method taking into account the fault size and the soil profile at the site. They concluded that *PGV* is better correlated with the occurrence of liquefaction than *PGA* and suggested that soil liquefaction is likely to occur when *PGV* exceeds 10–15 cm/s, which is supported by the observations (see Table I). *PGV* is obtained through integration of the ground acceleration time history. Integration by Fourier transform is utilized after filtering the original acceleration components with a band-pass filter between 0.05 and 33 Hz. The ground motion parameters considered in our proposal are also shown in the classification in Figure 3. Their efficiency is evaluated in the same manner as that of the other parameters and the results are illustrated in Figures 4(a) and 4(c).

The proposed method uses the *MIF* and *PGV* conditions in conjunction. Occurrence of liquefaction is judged as follows:

(1) If *PGV* is equal or larger than 10 cm/s and the total duration satisfying the condition $MIF_H \leqq 2/3$ Hz and $MIF_V \geqq 3$ Hz is equal or larger than 0.1 s, 'liquefaction' is detected. The index H denotes any of the horizontal components and the index V denotes the vertical component of the accelerogram.
(2) If *PGV* is equal or larger than 10 cm/s and the total duration satisfying the condition $MIF_H \leqq 1$ Hz and $MIF_V \geqq 3$ Hz is equal or more than 0.1 s, 'liquefaction suspicion' is detected. Indices H and V have the same meaning as in item 1).
(3) Otherwise, 'no liquefaction' is detected.

Table II. Relation between the method outputs and the comparison levels.

	Method of Suzuki	Method of Miyajima	Method of Ozaki and Takada	Proposed Method
Level 0	No liquefaction	Low possibility for liquefaction	No liquefaction	No liquefaction
Level 0.5	—	High possibility for liquefactionn	Possible liquefaction	Liquefaction suspicion
Level 1	Liquefaction	Very high possibility for liquefaction	Liquefaction	Liquefaction

6. COMPARISON OF LIQUEFACTION DETECTION METHODS

Performance of all methods is compared by processing the common data set. For the sake of comparison, we assumed that the different methods detect same levels of liquefaction occurrence. The levels are named 'Level 1', 'Level 0.5' and 'Level 0'. The relation between these levels and the outputs of the liquefaction detection methods is given in Table II.

The results of the detection for each record and method are shown in Table III and summarized in Figure 6. The judgments about the liquefied-site free-field records are shown in Figure 6(a). The method of Suzuki indicates the Port Island GL-16 record as Level 0 and the proposed method — as Level 0.5. This is due to the high-frequency content in the horizontal components that result in smaller $T_{z,a}$ and larger MIF_H values. The small value of the decrease rate of the predominant frequency causes the method of Miyajima to identify the Higashi-Kobe bridge record as Level 0.5. Same level is judged for the Hachirogata record due to low $A_{V,max}/A_{H,max}$. The method of Ozaki and Takada recognizes around half of the LF records as Level 1 and the rest as Level 0.5. Since this method uses only one parameter, its thresholds might need additional adjustment.

Figure 6(b) displays the judgments about the liquefied-site structure records. Both the method of Suzuki and the proposed method identify the Kawagishi-cho record as Level 0. While the former method estimates small D_c value, the latter method does not recognize it because the vertical acceleration component lacks of high-frequency content. Reason for that lack may be an effect of soil–structure interaction or an inability of the employed SMAC-A seismometer to record high frequencies. The method of Ozaki and Takada detects all these records as Level 1. The method of method of Miyajima gives either Level 0.5 or Level 1 judgments.

The results about the suspicious-site free-field records are shown in Figure 6(c). Two of them, Port Island GL-32 from the 1995 Hyogoken-Nanbu earthquake and Kushiro-G from the 1993 Kushiro-Oki earthquake, are detected by the method of Suzuki as Level 0 again due to smaller $T_{z,a}$ value. The Treasure Island record is identified as Level 1 by the methods of Miyajima and the proposed one, as the Takatori station record by the method of Ozaki and Takada. Remain four SF records are indicated as Level 0.5 by the methods of Miyajima and Ozaki and Takada. Note that the Kushiro-G record, at which site cyclic mobility was confirmed [25], is judged as Level 0.5 from all three-level methods.

Figure 6(d) depicts the detection of the non-liquefied-site free-field records. The methods of Suzuki and the proposed one recognize 90 per cent of these records as Level 0 while the

Table III. Judgments about occurrence of liquefaction.

No.	Site	Record group	Method of Suzuki	Method of Miyajima	Method of Ozaki and Takada	Proposed method
1	Kawagishi-cho	LS	0	1	1	0
2	Aomori Harbor	LF	1	1	1	1
3	Hachinohe Harbor	NF	0	0.5	0.5	0
4	Muroran Harbor	NF	0	0	0	0
5	Shiogama Harbor	NF	0	0	0.5	0
6	Akita-S	NF	0	1	0.5	0
7	Hachirogata	LF	1	0.5	1	1
8	C. de Abastos Frigorifico	NF	1	0	1	0
9	Caleta de Campo	NF	0	0	0	0
10	SC&T	NF	1	0	1	0
11	Tacubaya, D.F.	NF	0	0.5	1	0
12	Tlahuac Bombas	NF	1	0	1	0
13	Wildlife GL	LF	1	1	0.5	1
14	Wildlife GL-7.5	NF	0	1	0	0.5
15	Chiba Array, IIS	NF	0	0	0	0
16	Katsuura (KT552), NIED	NF	0	0	0	0
17	Kisarazu (KT521), NIED	NF	0	0	0	0
18	Mobara, Stokogyo	NF	0	0	0	0
19	Narashino, Takenaka ED	NF	0	0	0	0
20	Agnew, Agnews State Hospital	NF	0	0.5	0.5	0.5
21	Capitola, Fire Station	NF	0	0.5	0	0
22	Corralitos, Eureka Canyon Rd.	NF	0	0	0	0
23	Emeryville, 6363 Christie Ave	NF	1	0.5	1	0.5
24	Foster City, Redwood Shores	NF	0	0.5	0.5	0.5
25	Gilroy #1, Gavilan College	NF	0	0	0	0
26	Hollister, South St and Pine Drive	NF	0	0.5	0.5	0
27	Santa Cruz, UCSC/Lick Lab.	NF	0	0	0	0
28	Saratoga, Aloha Ave.	NF	0	0	0	0
29	SF, International Airport	NF	0	0	0	0
30	SF, Presidio	NF	0	0	0	0
31	Treasure Island	SF	1	1	0.5	1
32	Hanasaki-F	NF	0	0	0	0
33	Kushiro, JMA	NF	0	0	0	0
34	Kushiro-G	SF	0	0.5	0.5	0.5
35	Kushiro-GB	NF	0	0	0	0
36	Nemuro, JMA	NF	0	0	0	0
37	Tokachi-M	NF	0	0	0	0
38	Urakawa, JMA	NF	0	0	0	0
39	Urakawa-S	NF	0	0	0	0
40	Hakodate-F	NF	1	0.5	0.5	0
41	Hakodate-FB	NF	0	1	0.5	0
42	Hakodate-M	NF	0	0.5	0.5	0
43	Suttsu, JMA	NF	0	0	0	0
44	LA, Bell Postal Facility, Ground	NF	0	0	0	0
45	LA, Griffith Observatory	NF	0	0	0	0
46	LA, Sepulveda Canyon, Ground	NF	0	0	0	0
47	LA, Wadsworth VA Hosp., South Site	NF	0	0	0	0
48	Newhall, LA County Fire Station	NF	0	0.5	0	0.5
49	Pasadena, 535 South Wilson Ave.	NF	0	0	0	0

Table III. *Contd.*

No.	Site	Record group	Method of Suzuki	Method of Miyajima	Method of Ozaki and Takada	Proposed method
50	Tarzana, Cedar Hill Nursery	NF	0	0	0	0
51	Topanga, Fire Station, Ground	NF	0	0	0	0
52	Santa Monica City Hall, Ground	NF	0	0	0	0
53	Sylmar County Hospital	NF	0	0	0	0
54	Kushiro, JMA	NF	0	0	0	0
55	Nemuro, JMA	NF	0	0	0	0
56	Tomakomai, JMA	NF	0	0.5	0	0
57	Urakawa, JMA	NF	0	0.5	0	0
58	Hachinohe, JMA	NF	0	0	0	0
59	Amagasaki Bridge GR-2	SF	1	0.5	0.5	1
60	Amagasaki-G	LF	1	1	0.5	1
61	Amagasaki No.3 P.P., KE	LF	1	1	0.5	1
62	General Tech. Research Inst. GL, KE	NF	1	0.5	0	0
63	Higashi-Kobe Bridge	LF	1	0.5	1	1
64	Inagawa GR-1, PWRI	NF	0	0	0	0
65	Kobe, JMA	NF	0	0.5	0	0
66	Kobe-Dai8-G	LS	1	0.5	1	0.5
67	Kobe-JI-S	LF	1	1	0.5	1
68	Kobe University, CEORKA	NF	0	0	0.5	0
69	JR Nishi Akashi Station	NF	0	0	0	0
70	Port Island GL	LF	1	1	1	1
71	Port Island GL-16	LF	0	1	0.5	0.5
72	Port Island GL-32	SF	0	0.5	0.5	0.5
73	Port Island GL-83	NF	0	0	0	0
74	Rokko Island City, B3, B1F	LS	1	0.5	1	1
75	Shin Kobe S.S., KE	NF	0	0	0	0
76	Tadaoka, CEORKA	NF	0	0.5	0	0
77	JR Takarazuka Station	NF	0	0	0	0
78	JR Takatori Station	SF	1	0.5	1	0.5
79	Yotsubahsi GR-1, PWRI	NF	0	0.5	0.5	1
80	Akune (KGS004)	NF	0	0	0	0
81	Miyanojoh (KGS005)	NF	0	0	0	0
82	Ohkuchi (KGS003)	NF	0	0	0	0
83	Sendai (KGS007)	NF	0	0	0	0

methods of Miyajima and Ozaki and Takada identify around 75 per cent of them. The record at Tachibuya D. F. from the 1985 Michoacan, Mexico City earthquake is judged as Level 1 by the method of Ozaki and Takada though *PGA* at this site is equal to 37 cm/s^2. This low level of ground shaking implies that the liquefaction occurrence is unlikely. The judgment would be correct if an amplitude parameter has been used in addition to the energy one. It should be also noted that all methods interpret the record at Emeryville, 6363 Christie Ave from the 1989 Loma Prieta earthquake as Level 1 or Level 0.5. The record from this soft-soil site exhibits low-cycle acceleration with no frequency drop in the horizontal components but relatively high-frequency content in the vertical component and it is believed to reflect possible soil–structure interaction effect [34]. The site was also close to area of considerable liquefaction [35].

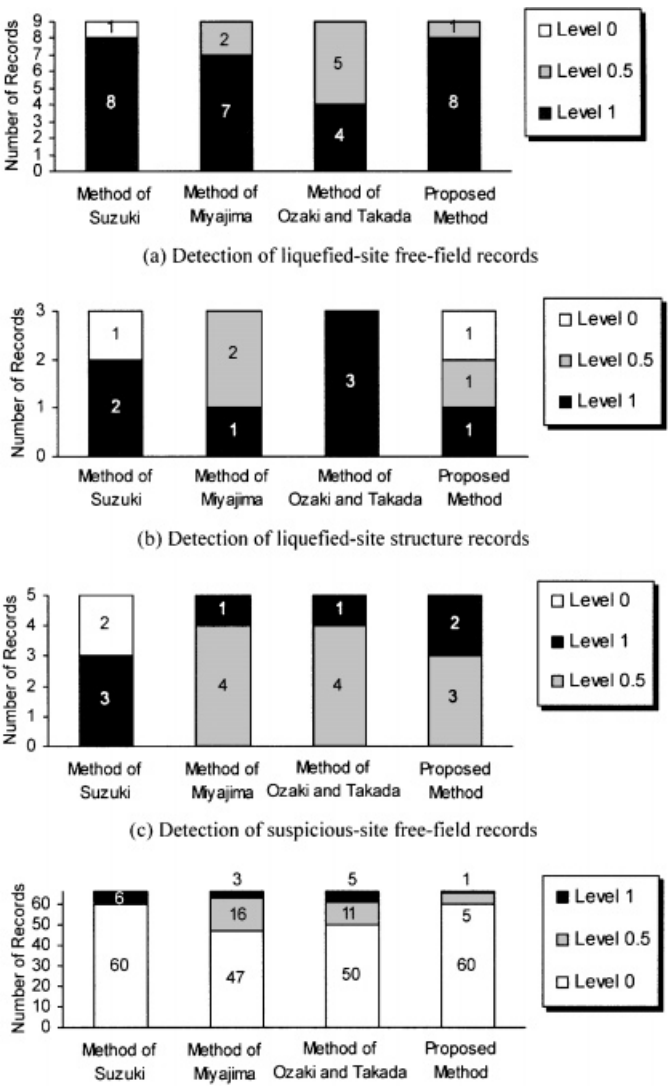

Figure 6. Detection of liquefaction occurrence by different methods.

7. CONCLUSIONS

Ability of the different types of ground motion parameters to indicate alone liquefaction occurrence is analysed and a new method for detection of liquefaction from the ground motion records is proposed. A comparative study on the performance of the different liquefaction detection methods is also conducted. The computations are carried out using a common data set of seismic records that are divided in four categories: liquefied-site free-field, liquefied-site

structure, suspicious-site free-field and non-liquefied-site free-field. From the results of this study the following conclusions are derived:

(1) Proposed method shows more efficient detection ability regarding the free-field records. It recognizes all liquefied and liquefaction-suspicious free-field records, as do the method of Miyajima and the method of Ozaki and Takada. In addition, proposed method identifies the most non-liquefied free-field records, nearly 90 per cent of them, as do the method of Suzuki.
(2) Most successful ground motion parameters for detection of liquefaction from seismic records are the frequency-related parameters that are time-dependent. Frequency alteration in the horizontal ground acceleration is the main indicator for the occurrence of liquefaction. Amplitude parameters show variable detection ability but seem to be an important part of the liquefaction detection methods in order to verify the intensity of the ground shaking. Energy parameters should be applied carefully since they reflect several characteristics of the ground motion and the effect of one parameter could obscure the effect of another.

There is still discussion which record can be considered from a liquefied site. In this paper, a classification of the recording sites with respect to liquefaction occurrence due to a particular earthquake is suggested. Opinion of the authors is that future records from liquefied sites might change some threshold values of the ground motion parameters used in the liquefaction detection methods.

ACKNOWLEDGEMENTS

The authors express their sincere gratitude to Prof. T. Suzuki and Prof. M. Miyajima, who kindly explained their methods in detail and to Dr K. Wakamatsu, who identified liquefaction occurrence at many sites. The strong motion records used in this study were provided by many institutions in Japan and the U.S.A. including these, mentioned in Section 3.

REFERENCES

1. Yamazaki F, Noda S, Meguro K. Developments of early earthquake damage assessments systems in Japan. *Structural Safety and Reliability — Proceedings of ICOSSAR'97*, *The 7th International Conference on Structural Safety and Reliability*, *Kyoto*, *24–28 November 1997*. Balkema: Rotterdam, 1998; 1573–1580.
2. Tsukamoto K, Morimoto I, Yoshihara Y, Orense R, Yasuda S. Estimation of liquefaction based on water elevation within a pipe. *Earthquake Geotechnical Engineering — Proceedings of IS-Tokyo'95*, *The 1st International Conference on Earthquake Geotechnical Engineering*, *Tokyo*, *14–16 November*. Balkema: Rotterdam, 1995.
3. Seed HB, Idriss IM. Simplified procedure for evaluating soil liquefaction potential. *Journal of the Soil Mechanics and Foundation Division*, *Proceedings of the ASCE* 1971; **97** (SM9): 1249–1273.
4. Midorikawa S, Wakamatsu K. Intensity of earthquake motion at liquefied sites. *Soils and Foundations*, 1988; **28** (2): 73–84.
5. Kayen RE, Mitchell JK. Assessment of liquefaction potential during earthquakes by Arias intensity. *Journal of Geotechnical and Geoenvironmental Engineering* 1997; **123**(12): 1162–1174.
6. Towhata I, Park JK, Orense RP, Kano H. Use of spectrum intensity for immediate detection of subsoil liquefaction. *Soils and Foundations* 1996; **36**(2): 29–44.
7. Suzuki T, Shimizu Y, Nakayama W. Characteristics of strong motion records at the liquefied sites and judgment for liquefaction. *11th European Conference on Earthquake Engineering*, Paris, France, 6–11 September, CD-ROM. Balkema: Rotterdam, 1998.
8. Miyajima M, Nozu S, Kitaura M. A detection method for liquefaction using strong motion records. *Proceedings of 24th JSCE Earthquake Engineering Symposium*, Kobe, 24–26 July. JSCE, 1997; 265–268 (in Japanese).

9. Takada S, Ozaki R. A judgment for liquefaction based on strong ground motion. *Proceedings of 24th JSCE Earthquake Engineering Symposium*, Kobe, 24–26 July. JSCE, 1997; 261–264 (in Japanese).
10. Nakayama W, Shimizu Y, Suzuki T, A new method to detect subsoil liquefaction using seismic records. *Proceedings of the 53rd Annual Conference of Japanese Society of Civil Engineers*, vol. 1-B. JSCE, 1998; 862–863 (in Japanese).
11. Miyajima M, Kitaura M, Nozu S. Detective method of liquefaction using strong ground motion records. *Proceedings of the 3rd China-Japan-US Trilateral Symposium on Lifeline Earthquake Engineering*, Kunming, China, August 1998; 133–140.
12. Ozaki R. Study on real-time earthquake mitigation — liquefaction monitoring and earthquake countermeasures. *PhD Thesis*, Kobe University, 1999 (in Japanese).
13. Shimizu Y, Watanabe A, Koganemaru K, Nakayama W, Yamazaki F. Super high-density real-time disaster mitigation system. *12th World Conference on Earthquake Engineering*, *Auckland*, *New Zealand*, *30 January–4 February*, CD-ROM, Paper No. 2345. New Zealand Society for Earthquake Engineering, 2000.
14. Yamamoto M, Nozu S, Miyajima M, Kitaura M. Proposal for liquefaction indices and their verification. *Proceedings of 25th JSCE Earthquake Engineering Symposium*, *Tokyo*, *29–31 July*. JSCE, 1999; 417–420 (in Japanese).
15. Arias A. A measure of earthquake intensity. In *Seismic Design for Nuclear Power Plants*, Hansen RJ (ed.). MIT Press: Cambridge, MA, 1970.
16. Seed HB, Tokimatsu K, Harder LF, Chung RM. Influence of SPT procedures in soil liquefaction resistance evaluation. *Journal of Geotechnical Engineering* 1985; **111**(12): 1425–1445.
17. Kramer S. *Geotechnical Earthquake Engineering*. Prentice-Hall: Upper Saddle River, NJ, 1996.
18. National Oceanic and Atmospheric Administration. *Earthquake Strong Motion CD-ROM*. National Geophysical Data Center: Boulder, CO, 1989.
19. *Niigata Earthquake Disaster Investigation Report*. Japanese Geotechnical Society, 1964 (in Japanese).
20. Bureau for Ports and Harbours, Ministry of Transport and Hokkaido Development Bureau, *Damage to Harbour Structures by the 1968 Tokachi-Oki Earthquake*. Hokkaido Development Agency, 1968 (in Japanese).
21. Yanagisawa E, Ishihara K, Tobita Y, Nakamura S. On the vibration characteristics of front dike of Hachirogata reclamation in relation to the Nihonkai-Chibu earthquake. *Tsuchi-to Kiso* 1984; **32**(9): 41–44 (in Japanese).
22. Holzer TL, Youd TL, Hanks TC. Dynamics of liquefaction during the 1987 Superstition Hills, California, earthquake. *Science* 1989; **244**; 56–59.
23. Darragh RB, Shakal AF, The site response of two rock and soil station pairs to strong and weak ground motion. *Bulletin of the Seismological Society of America* 1991; **81**(5): 1885–1899.
24. Iai S, Morita T, Kameoka T, Matsunaga Y, Abiko K. Response of a dense sand deposit during 1993 Kushiro-Oki earthquake. *Soils and Foundations* 1995; **35**(1): 115–131.
25. Sato Y, Ichii K, Hoshino Y, Sato Y, Miyata M, Morita T, Iai S. Strong-motion earthquake records on the 1995 Hyogoken Nanbu earthquake in port areas. *Technical Note of the Port and Harbour Research Institute*, Ministry of Transport, Japan, Vol. 907, 1998.
26. Editorial Committee for the Report on the Hanshin-Awaji Earthquake Disaster. *Report on the Hanshin-Awaji Earthquake Disaster*, General issues vol. 2, 1998 (in Japanese).
27. Hagiwara R, Tamura K, Honda R, Usami J. Earthquake and earthquake ground motion. Report on the disaster caused by the 1995 Hyogoken Nanbu earthquake. *Journal of Research PWRI* 1997; **33**: 5–14.
28. Inagaki H, Iai S, Sugano T, Yamazaki H, Inatomi T. Performance of caisson type quay walls at Kobe port. *Soils and Foundations — Special Issue* 1996; 119–136.
29. Hamada M, Isoyama R, Wakamatsu K, *The 1995 Hyogoken-Nanbu* (*Kobe*) *Earthquake — Liquefaction*, *Ground Displacement and Soil Condition in Hanshin Area*. Association for Development of Earthquake Prediction: Japan, 1995.
30. Shibata T, Oka F, Ozawa Y. Characteristics of ground deformation due to liquefaction. *Soils and Foundations – Special Issue* 1996; 65–79.
31. Yamazaki F, Ansary MA, Towhata I. Application of a dynamic effective stress model at the reclaimed site during the Great Hanshin earthquake, 1995. *Earthquake Geotechnical Engineering — Proceedings of IS-Tokyo'95*, *The 1st International Conference on Earthquake Geotechnical Engineering*, Tokyo, 14–16 November. Balkema: Rotterdam, 1995.
32. Jarpe SP, Hutchings LJ, Hauk TF, Shakal AF. Selected strong- and weak-motion data from the Loma Prieta earthquake sequence. *Seismological Research Letters* 1989; **60**(4): 167–176.
33. Qian Sh, Chen D. *Joint Time-Frequency Analysis: Methods and Applications*. Prentice-Hall PTR: Upper Saddle River, NJ, 1996.
34. Idriss JM. Response of soft soil sites during earthquakes. In *H. Bolton Seed — Memorial Symposium Proceedings*, Duncan JM (ed.). BiTech: Vancouver, BC, 1990.
35. The Governor's Board of Inquiry on the 1989 Loma Prieta Earthquake. *Competing Against Time*. Office of Planning and Research, CA, 1990.

